Experimental Microkinetic Approach of the Photocatalytic Oxidation of Isopropyl Alcohol on TiO_2. Part 2. From the Surface Elementary Steps to the Rates of Oxidation of the C_3H_xO Species

F. Arsac, D. Bianchi,* J. M. Chovelon, C. Ferronato, and J. M. Herrmann

Laboratoire d'Application de la Chimie à l'Environnement (LACE), UMR 5634, Université Claude Bernard, Lyon-1, Bat. Raulin, 43 Bd du 11 Novembre 1918, 69622 Villeurbanne-France

Received: December 12, 2005; In Final Form: January 22, 2006

The present study concerns an experimental microkinetic approach of the photocatalytic oxidation (PCO) of isopropyl alcohol (IPA) into acetone on a pure anatase TiO_2 solid according to a procedure previously developed. Mainly, the kinetic parameters of each surface elementary step of a plausible kinetic model of the PCO of IPA are experimentally determined: natures and amounts of the adsorbed species and rate constants (preexponential factors and activation energies). These kinetic parameters are used to evaluate a priori the catalytic activity (turnover frequency, TOF, in s^{-1}) of the solid that is compared to the experimental value. The kinetics parameters are obtained by using experiments in the transient regime with either a FTIR or a mass spectrometer as a detector. The microkinetic study shows that only strongly adsorbed IPA species (two species denoted nd-IPA_{sads} and d-IPA_{sads} due to non- and dissociative chemisorption of IPA respectively) are involved in the PCO of IPA. A strong competitive chemisorption between IPA_{sads} and a strongly adsorbed acetone species controls the high selectivity in acetone of the PCO at a high coverage of the surface by IPA_{sads}. The apparent rate constant ($1.4\ 10^{-3}\ s^{-1}$) of the Langmuir−Hinshelwood elementary step between IPA_{sads} and the active oxygen containing species generated by the UV irradiation provides the TOF of the PCO for IPA/O_2 gas mixtures. The kinetic parameters of the elementary steps determined by the experimental microkinetic approach allow us to provide a reasonable simulation of the experimental data (coverages of the adsorbed species and partial pressures of the gases of interest) recorded during a static PCO of IPA_{sads} species.

I. Introduction

The objective of the microkinetic approach of a gas−solid catalytic process is to correlate the kinetic parameters of the surface elementary steps involved in a kinetic model of the reaction to macroscopic kinetic parameters such as the turnover frequency (denoted TOF) and its evolution with experimental parameters (reaction temperature, partial pressures of the reactants).[1] The kinetic parameters of the elementary steps can be either determined by theoretical calculation (ex: DFT) or by using experimental procedures.[1] In previous studies, we have developed the experimental microkinetic approach (denoted EMA) considering two catalytic processes involving reactants with simple molecular structures (a) the CO/O_2 reaction on Pt/Al_2O_3 catalysts[2,3] and (b) the catalytic oxidation of a diesel soot formed in the presence of a cerium containing additive.[4−6] However, the relative simplicity of the reactants limits the number of surface elementary steps involved in the kinetic model of the reaction. This explains that we have undertook,[7] the EMA of the deep (formation of CO_2 and H_2O) photocatalytic oxidation of isopropyl alcohol on a TiO_2 solid (from Millennium, BET = 350 m^2/g) to consider a reactant with a complex structure. From the viewpoint of the EMA, the interest of this reaction is that it is performed at 300 K. At this temperature, the rates of elementary steps such as the desorption of the reactants and intermediates species are low, leading to a significant simplification of the calculations linked to the TOF.

The first stage of the EMA is to adopt a plausible kinetic model of the reaction. This has been made in part 1[7] of the present study considering literature data[8,9] on the mechanism of the O_2−PCO of IPA. The kinetic model (denoted M1) supporting the study is[7]

S1: adsorption of IPA $IPA_g \rightarrow IPA_{ads}$

S2: desorption of IPA $IPA_{ads} \rightarrow IPA_g$

S3: adsorption of O_2 $O_2 \rightarrow O_{2\ ads} \rightarrow 2\ O_{ads}$

S4: desorption of O_2 $2O_{ads} \rightarrow O_2$

S5: UV formation of the reactive species

$$TiO_2 + h\nu + O_{2ads}\ (\text{or}\ O_{ads}) \rightarrow X_{ads}^*$$

S6: first Langmuir−Hinshelwood (L−H) step

$$IPA_{ads} + X_{ads}^* \rightarrow I_{1ads} + \Sigma\, Y_{ads}$$

S7: desorption of I_{1ads} $I_{1ads} \rightarrow I_{1g}$

S8: second L−H step $I_{1ads} + X_{ads}^* \rightarrow I_{2ads} + \Sigma\, Y_{ads}$

The addition of successive elementary steps similar to S7−S8 completes the mechanism for the deep oxidation of IPA (CO_2 and H_2O formation).[7] In steps S6 and S8, ΣY_{ads} represents adsorbed species with a composition and a charge allowing to respect the conservation of atoms and charges. Several kinetic parameters of the elementary steps of model M1 have been studied in part 1 of the present study.[7] In particular, it has been

* To whom correspondence should be addressed. E-mail: daniel.bianchi@univ-lyon1.fr.

10.1021/jp057255p CCC: $33.50
Published on Web 03/07/2006

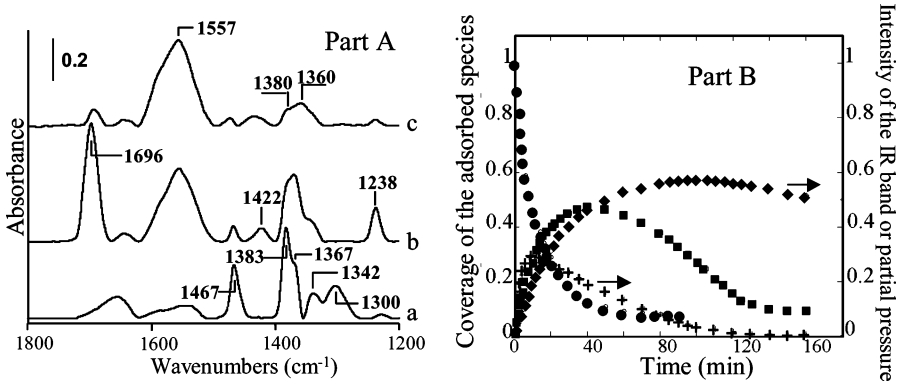

Figure 1. FTIR study of the static O_2-PCO ($P_{O2} = 1.9\ 10^4$ Pa) of the IPA_{sads} species. Part A: Evolution of the FTIR spectra of the adsorbed species with the duration T.I of the O_2-PCO; (a−c) TI = 0, 30, and 120 min. Part B: (● and ■) Coverages of the IPA_{sads} and Ac_{sads} species respectively; (+) Partial pressure (Torr) of acetone; (◆) Intensity of the IR band at 1557 cm^{-1} (formate species).

shown in agreement with literature data[8−13] that the I_{1ads} intermediate species is an adsorbed acetone molecule (denoted Ac_{ads}) and that it is the single route to the CO_2 formation from IPA.[7] This explains that we have considered the EMA of the PCO of IPA into acetone as the first stage of the deep PCO of IPA. Moreover, it has been shown that IPA is strongly adsorbed (step S1) forming two adsorbed species without and with dissociation of IPA (adsorbed species denoted nd- and d- IPA_{sads}, respectively) allowing us to develop the EMA of the reaction in the absence of gaseous IPA via the O_2-PCO of the IPA_{sads} species (PCO of IPA_{sads} has been also performed in the absence of O_2 via the oxygen lattice of TiO_2, denoted $O_{lat}-PCO$).[7] It has been shown that a key surface process of the PCO of IPA is the competitive chemisorption between IPA_{sads} and Ac_{ads} species (the competition with the product H_2O is not significant).[7] On a clean TiO_2 surface, (a) the reactant IPA is strongly adsorbed on a large number of sites (denoted s_1), 948 μmol/g, and (b) the product acetone is adsorbed (a single strongly adsorbed species denoted Ac_{sads}) mainly of on a fraction of the s1 sites, 440 μmol/g.[7] The heat of adsorption of IPA is strongly higher than that of acetone explaining that the competitive chemisorption on the common s_1 sites is in favor of IPA.[7] However, there is a small amount of the TiO_2 sites (denoted s_2) that are specific to the adsorption of acetone (there is no competition with IPA), ≈32 μmol/g.[7] At high coverage of the surface by IPA_{sads}, only these sites may allows the deep oxidation of IPA: on the other sites the transformation of IPA_{sads} must be followed by the fast desorption of acetone.[7]

In the present part 2 of the EMA of the PCO of IPA into acetone (a) we provide additional quantitative experimental kinetic data on the elementary step S6 in particular considering experimental conditions for the PCO of IPA/O_2 gas mixtures and (b) we present a modeling of macroscopic kinetic data: the evolutions of the coverages of the adsorbed species and the concentration of gaseous species during the static O_2-PCO of IPA_{sads} and the turnover frequency of the PCO of IPA_g/O_2.

II. Experimental Section

The TiO_2 catalyst (PC 500 from Millenium, pure anatase, BET: 335 m^2/g) and the pretreatment procedures have been described in detail in part 1.[7] Two analytical systems described in detail in part 1[7] have been used to characterize (a) the natures and the amounts of the adsorbed species formed by adsorption of IPA and acetone on the TiO_2 surface as well as their evolutions during the O_2-PCO and (b) the kinetic parameters of the elementary steps of model M1. Mainly, the first analytical system allowed us to study (a) the modification of the adsorbed species on a TiO_2 pellet ($\Phi = 18$ mm, $m = 70$ mg) and (b) the composition of the gas phase during static O_2-PCO by using an IR cell (quartz and Pyrex, grease free, FTIR spectrometer: Brucker IFS-28). The second analytical system[7] was designed to perform experiments in the transient regime (i.e., isothermal adsorption and desorption, oxidation under UV irradiation (PCO) and in the dark, temperature programmed desorption and oxidation) with a mass spectrometer (denoted M.S) as a detector. Mainly, various valves allowed us to perform controlled switches between regulated gas flows in the range 100−1000 cm^3/min (at the atmospheric pressure), which passed through the TiO_2 sample ($m = 0.208$ g) contained in a quartz microreactor (volume of ≈2.5 cm^3).

III. Results

The EMA developed in the present part 2 concerns mainly step S6 of the kinetic model. However, to facilitate the presentation, we summarize few results of part 1.

3.1. Coverage of TiO_2 and Acetone Production during Static O_2-PCO of IPA_{sads} using FTIR. It has been shown that step S1 forms strongly adsorbed species, allowing to develop the EMA via the O_2-PCO of IPA_{sads}.[7] For instance, spectrum a in Figure 1A corresponds the IPA_{sads} species (two adsorbed species denoted nd- and d-IPA_{sads} due to nondissociative and dissociative chemisorption of IPA, respectively).[7] The evolutions of the IPA_{sads} species during static O_2-PCO is followed by using the intensity of the IR band at 1467 cm^{-1} that is (a) common to the two IPA species and (b) not strongly overlapped with the IR bands of the new adsorbed species formed by step S6. The O_2-PCO of IPA_{sads} (performed with $P_{O_2} = 1.9 \times 10^4$ Pa in Figure 1) is studied by repeating the following cycle: (a) the TiO_2 pellet is positioned in front of the UV lamp for an irradiation duration t_i and (b) then it is positioned on the IR beam to study the modification of the adsorbed species on the TiO_2 surface. After each period t_i, the composition of the gas phase in the IR cell is determined by FTIR. Figure 1, part A, shows the evolutions of the FTIR spectra with the total irradiation duration: $TI = \Sigma\, t_i$. It can be observed that the IR bands of IPA_{sads} (i.e., 1467 cm^{-1}) decrease progressively with the increase in TI (spectra a and b), whereas in parallel, new IR bands increase in particular that at 1696 cm^{-1} (spectrum b) ascribed to strongly adsorbed acetone species (Ac_{sads}).[7] This IR band increases during 40 min and then decreases progressively leading to spectrum c that is dominated by an IR band at 1557 cm^{-1} (spectra b and c) that has been ascribed to formate species.[7,13−15] Curves ● and ■ in Figure 1B show the evolutions with TI of θ_I and θ_A the coverages of IPA_{sads} and Ac_{sads}. The

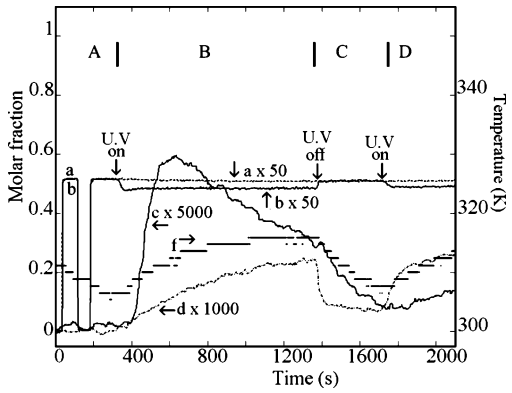

Figure 2. Evolutions of the molar fractions of the gases during transient experiments linked to the O_2−PCO of IPA_{sads} on TiO_2 using 1% O_2/1%Ar/He mixture: Part A: adsorption and desorption of O_2 after formation of IPA_{sads} (see Figure 2); parts B and D: O_2−PCO of IPA_{sads}; part C: without UV irradiation. (a) Ar, (b) O_2, (c) acetone, (d) CO_2, and (f) temperature of the TiO_2 sample.

θ_I and θ_A values are obtained using the ratios $\theta_I = [A(1467\ cm^{-1})$ at TI$]/[A(1467\ cm^{-1})$ at TI $= 0]$ and $\theta_A = [A(1696\ cm^{-1})$ at TI$]/[A(1696\ cm^{-1})$ measured after adsorption of Ac_g on a clean TiO_2 surface].[7] The decrease of θ_I indicates the transformation of IPA_{sads} according to step S6, whereas the profile of θ_A with a maximum at TI = 40 min is that expected for an adsorbed intermediate species in successive reactions.[16,17] Curve ◆ in Figure 1B provides the evolution of the intensity of the IR band at 1557 cm^{-1}: it indicates that the "formate" species are also intermediates species of the PCO (for the CO_2 production). Curve + in Figure 1B, provides the evolution of the partial pressure of Ac: P_{Ag}, in the IR cell during the static O_2−PCO of IPA_{sads}. It indicates that a significant fraction of acetone desorbs during the first minutes of the reaction (at high coverage of IPA_{sads}) before its consumption. Note that the maximum in P_{Ag} is at a TI value lower than that of the maximum of θ_A. This is clearly unexpected considering the plausible kinetic model M1 because the formations of Ac_{sads} (step S6) and of Ac_g (step S7) are successive. This means that some elementary steps of model M1 must be modified considering these experimental observations. One of the intent of the present EMA is to simulate the experimental data in Figure 1B by using a modified version of the kinetic model M1. The impacts of the experimental conditions (partial pressures of O_2 and H_2O) on the O_2−PCO of IPA_{sads} have been studied leading to the conclusions that (a) $P_{O_2} > 1.9$ kPa and $P_{H_2O} > 395$ Pa have no significant impact on the rate of disappearance of IPA_{sads}.[7]

3.2. Study of Step S6 during O_2−PCO of IPA_{sads} by using MS. FTIR spectroscopy[7] provides experimental data neither on the oxygen consumption nor on the amount of adsorbed species: these parameters have been measured in the present study with the MS system. After the formation of the IPA_{sads} species (see Figure 2 in ref 7) a switch He → 1% O_2/1%Ar/ He is performed at 300 K as shown Figure 2, part A. It is observed neither a oxygen consumption nor a desorption/formation of gaseous compounds confirming the absence of desorption/oxidation of IPA_{sads} in the absence of UV light. After a switch 1% O_2/1% Ar/He → He confirming the absence of desorption of O_2, the O_2 containing mixture is again introduced and the UV lamp is turned on (Figure 2, part B) to perform the O_2−PCO of IPA_{sads}. It can be observed that there is an immediate oxygen consumption, whereas the acetone production (Figure 2, curve c) increases strongly after a short delay from the O_2 consumption: 95 s. This observation is consistent with that of Larson et al.,[11] who have performed similar experiments by using a 0.15% O_2-containing gas flow. The CO_2 production starts at the appearance of gaseous acetone and increases progressively with time on stream (Figure 2 curve d) without CO production (taking into account the sensitivity of the analytical procedure). The oxygen consumption (difference between curves a and b) changes progressively with time on steam from 12.6 to 9.6 μmol of O_2/(g min) for 1 and 17 min of O_2−PCO, respectively. This change is probably associated with the modification of the coverage of the TiO_2 surface from mainly IPA_{sads} to a mixture of IPA_{sads}, Ac_{sads} and formate species (Figure 1) that have different reactivities. Note that the acetone production decreases with time on stream, whereas that of CO_2 increases: this is due to the fact that in the course of the O_2−PCO more acetone can be adsorbed on the sites liberated by the oxidation of IPA_{sads}. The rate at the maximum of the acetone production in Figure 2 is 2.36 μmol/(g·min) strongly higher than that measured during O_{lat}−PCO of IPA_{sad},[7] 0.23 μmol/(g·min), indicating that O_2 allows us to produce and to maintain a higher amount of X^*_{ads} species. This impact of O_2 on the initial rate of the acetone formation has been also observed by Larson et al.:[11] ≈0.6 and 0.045 μmol/(g·min) with 0.15% and 30 ppm of O_2-containing gas mixtures. The delay of 95 s between the consumption of O_2 and the appearance of acetone when the UV lamp is turned on indicates that there is an accumulation of oxygen containing species on the TiO_2 surface. Considering the rate of O_2 consumption, 12.6 μmol/(g·min), this indicates that ≈20 μmol of O_2/g have been fixed on the surface. Assuming the transformation of nd-IPA_{sads} into Ac_{ads}, $C_3H_8OH_{sads}$ + 1/2 $O_2 \rightarrow C_3H_6O_{sads} + H_2O$, the oxygen fixed on TiO_2 corresponds to 40 μmol/g of Ac_{ads} that is a value consistent with the number of s_2 sites specific to the acetone adsorption (without competition with IPA): 32 μmol/g determined previously.[7] Note that the temperature of the TiO_2 sample (Figure 2, curve f) increases slightly during the O_2−PCO to a pseudo stationary value. After 1040 s of O_2−PCO, the UV lamp is turned off (Figure 2, part C) leading to (a) the immediate cut off of the O_2 consumption (curve b), (b) the sharp decrease in the CO_2 production (curve d), (c) a more progressive decrease in the acetone production (curve c) due to the desorption of Ac_{ads} accumulated on the s_1 sites in the presence of the remaining IPA_{sads} species, and (d) the immediate decrease in the temperature (curve f). The abrupt decrease in CO_2 indicates that a large fraction of its production is strongly linked to the O_2 activation under UV irradiation either the rate of desorption of the adsorbed precursor of CO_2 is very high or CO_{2g} is formed directly from the O_2−PCO of an adsorbed species (i.e., from Ac_{sads}). The slight residual CO_2 formation in the dark is probably linked to the desorption of adsorbed species (i.e., formate, carboxylate). This seems to support the view that there are several routes for the CO_2 formation from acetone.

Before the UV lamp is turned off in Figure 2B (after 1040 s of O_2−PCO of IPA_{sads}), the rates (in μmol/(g·min)) of the different processes are CO_2 production = 2.9, O_2 consumption = 9.5, and acetone formation = 1.2, indicating from the oxygen mass balance that the O_2 consumption is still linked to the accumulation of strongly adsorbed oxygen containing species before their finale oxidation in CO_2. This is consistent with the increase of Ac_{sads} and formate species on the TiO_2 surface as observed in Figure 1. In Figure 2D, the UV lamp is again turned on: it can be observed that (a) the O_2 consumption starts immediately and (b) the CO_2 production increases more rapidly than during the first O_2−PCO (Figure 2B) because of the fact that there is Ac_{sads} species (in Figure 2B, Ac_{sads} are formed only

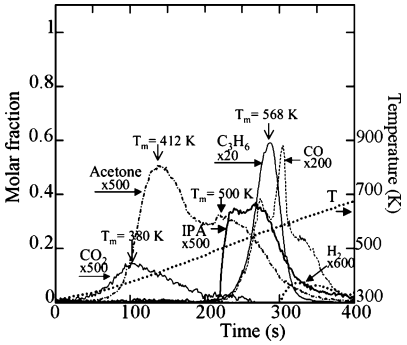

Figure 3. Temperature programmed desorption of the strongly adsorbed species formed after 30 min of O_2-PCO of IPA_{sads} at 300 K.

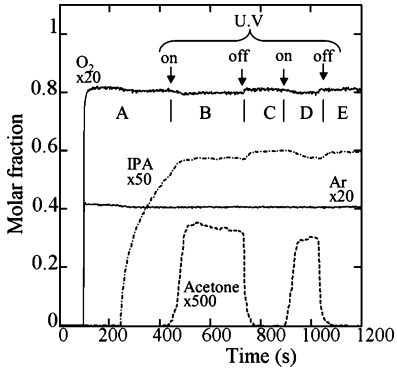

Figure 4. Evolutions of the molar fractions of the gases during transient experiments linked to the O_2-PCO of IPA_g at 300 K using a 1.2% IPA/ 4%O_2/2%Ar/He gas mixture. Part A: Adsorption of IPA in the absence of UV light; parts B and D: O_2-PCO with the UV lamp turned on; parts C and D: the UV lamp is turned off.

after the significant removal of IPA_{sads} due to the competitive chemisorption). Moreover, the higher rate of CO_2 production during the first minutes of Figure 2D as compared to the first minutes of Figure 2B (whereas the amount of IPA_{sads} must be lower in part D) confirms clearly that (a) the intermediate species of the CO_2 production must be formed and (b) there is not a faster route from IPA_{sads} to CO_2 than acetone formation. The acetone production increases more progressively in part D of Figure 2 than in part B, because (a) a fraction of the Ac_{ads} species has been desorbed in part C and (b) there is a larger amount of free s_1 sites for the formation of Ac_{sads} due to the removal of IPA_{sads}. It must be noted in Figure 2 that when the UV lamp is turned off and on there are neither an overshoot in the O_2 signal (i.e., there is no significant O_2 desorption) nor an extra O_2 consumption (i.e., readsorption of O_2). This indicates that (a) the amount of the X_{ads}* species involved in the O_2-PCO (formed under UV− irradiation) is very low and (b) in the presence of O_2 there is no significant formation of O vacancies as compared to $O_{latt}-PCO$[7] (the color of TiO_2 remains white). In summary, if O_{latt} species participate to the O_2-PCO,[11,18−20] the rate of reoxidation of the vacancies is very high and step S3 is not the limiting step of the PCO process.

The changes in the coverage of the adsorbed species due to O_2-PCO of IPA_{sads} have been studied performing a TPD in helium after a UV irradiation duration of 30 min as shown in Figure 3. In part 1,[7] it has been shown that the TPD of IPA_{sads} leads mainly to the formation of two broad peaks of IPA_g at 437 and 512 K and a sharp C_3H_6 peak at 564 K with a ratio $C_3H_6/IPA_g = 3.1$.[7] The comparison of the TPD peaks in Figure 3 with those observed previously[7] shows that O_2-PCO decreases significantly the amount of IPA_{sads} desorbing as IPA_g at low temperatures: the ratio C_3H_6/IPA_g increases from 3.1 to 20 and 34 after TI = 0, 30, and 61 min, respectively. This shows that there is a difference in the reactivity of the IPA_{sads} for the O_2-PCO: the adsorbed IPA species with the highest activation energy of desorption giving propylene (probably d-IPA_{sads}) are less reactive than the adsorbed species with a lower activation energy of desorption and desorbing as IPA_g (probably nd-IPA_{sads}). Moreover, Figure 3 confirms the accumulations on the TiO_2 surface of (a) acetone species (45 μmol/g) according to two peaks at T_m = 412 and 500 K and (b) weakly adsorbed species (i.e., carbonate, formate) desorbing as CO_2 with a TPD peak at 380 K: 10 μmol/g. This last peaks it linked to the remaining CO_2 production during the dark period in Figure 2, part C.

3.3. O_2-PCO in the Presence of IPA in the Gas Phase. These experimental conditions correspond to a classical catalytic reaction.

Measurement at the Steady State by using the MS. Figure 4A shows the evolutions of the M.Fs during the switch He → 1.2% IPA/4% O_2/2% Ar/He in the absence of UV irradiation. The observations are similar to those in the absence of O_2,[7] indicating that IPA_g forms IPA_{sads} (the MF of IPA is equal to 0 during several seconds) and IPA_{wads} species (progressive attainment of the adsorption equilibrium): there is neither acetone nor CO_2 formation (absence of oxidation in the dark). After 350 s of adsorption, the UV lamp is turned on leading to the immediate O_2 consumption, whereas the acetone production is slightly delayed. A pseudo steady state for the acetone production is observed after 85 s of UV irradiation: the rate of the acetone production R_{Acg} decreases slightly with time on stream as observed in Figure 4B. After 300 s, the UV lamps were turned off leading to the immediate decrease in the acetone production associated to the increase in the MF of IPA. Note the clear difference in the evolution of the acetone production when the UV light is turned off in Figure 4 (fast decrease in the presence of gaseous IPA) and Figure 3C (slow decrease in the absence of gaseous IPA). This is due to the strong competitive chemisorption between IPA and acetone on the s_1 sites in the presence of IPA_g. The partial pressure of IPA_g maintains $\theta_1 = 1$: Ac_{sads} can be absorbed only on the small amount of s_2 sites. When the UV lamp is turned on (Figure 4D) and off (Figure 4E) the acetone production increases and decreases immediately. The rates (in μmol/(g·min)) of the various processes at the end of Figure 4B (average values on 1 min of O_2-PCO) are (a) IPA consumption = 12.6; (b) acetone production = 12.6; and (c) oxygen consumption = 7. These values show that, at the pseudo steady state of the O_2-PCO of IPA_g, the IPA consumption is mainly linked to the acetone production. Bickley et al.[10] have a similar conclusion for the O_2-PCO of IPA_g: "alcohol dislodges acetone from the TiO_2 surface in a 1:1 molar ratio". The oxygen consumption is roughly equal (considering the accuracy of the measurement with the M.S) to that expected (6.3 μmol/(g·s)) for the transformation of IPA_g into Ac_g according to the global reaction $C_3H_8OH + {}^1/_2O_2 \rightarrow C_3H_6O + H_2O$. There is neither a strong accumulation of oxidized adsorbed species nor CO_2 formation during the O_2-PCO of IPA_g (at the difference of the O_2-PCO of IPA_{sads}) confirming that (a) there are no others routes to CO_2 that Ac_{sads} species and (b) the coverage of the TiO_2 surface is controlled by the competitive chemisorption IPA_{sads}/Ac_{sads}. In Figure 4B, the short delay in the appearance of Ac_g as compared to the O_2 consumption when the UV light is turned-on indicates a slight accumulation of Ac_{sads}, ≈17 μmol/g, corresponding probably to the s_2 sites as observed in Figure 2. The difference in the acetone accumulations in Figure 4B, 17 μmol/g, and

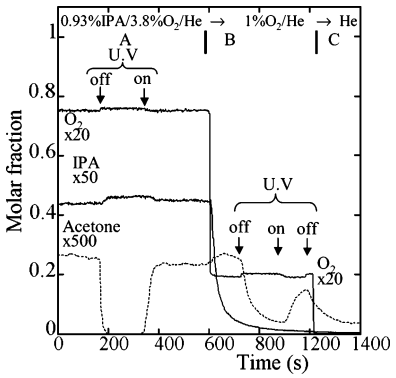

Figure 5. Evolutions of the molar fractions of the gases during transient experiments linked to the O_2-PCO of IPA_g at 300 K using a 0.93% IPA/3.8%O_2/He gas mixture. Part A: at the steady state of the O_2-PCO, the UV lamp turned on and off; part B: a switch 0.93% IPA/3.8%O_2/He → 1%O_2/He is performed and then the UV lamp is turned off and on; part C: a switch 1%O_2/He → He is performed with in the absence of UV irradiation.

Figure 2, 40 μmol/g, can be ascribed to the stronger competitive chemisorption between IPA_{sads} and Ac_{sads} on the s_1 sites in the presence of IPA_g that decrease the amount of Ac_{sads} diffusing from s_1 to s_2.

Experiments in the Transient Regime. Figure 5 shows the evolutions of the MFs at the outlet of the quartz microreactor according to several experiments in the transient regime to obtain more data on the elementary steps of model M1. The data in Figure 5A are similar to those in Figure 4 using a 0.98% IPA/3.8% O_2/2% Ar/He gas mixture: at the pseudo steady state of the PCO reaction the acetone production ceases and starts immediately when the UV lamp is turned off and on, respectively. Figure 5B shows the evolutions of the MFs during the switch 0.98% IPA/3.8%O_2/2%Ar/He → 1% O_2/2%Ar/ He performed under UV irradiation. It can be observed that during the first seconds of the switch the acetone production is strongly affected neither by the removal of the IPA_g (the M.F of IPA decreases progressively due to the desorption of the weakly adsorbed IPA species) nor by the change in P_{O_2}. The first observation means that (a) P_I has no impact on R_{Acg}; (b) the IPA_{wads} species is not significantly involved in the PCO reaction (its removal may explain the slight increase in R_{Acg} during the first second of the switch in Figure 5B); and (c) there is a reservoir of adsorbed intermediate species on TiO_2 for the acetone production, allowing to produce acetone at the same rate than at the steady state. This confirms that the IPA_{sads} species is the intermediate species of the O_2-PCO of IPA_g. The fact that R_{Acg} is independent of P_I is in agreement with the early observations of Bickley et al.,[10] who conclude that the kinetic order of IPA_g during O_2-PCO is 0 for $P_I > 42$ Pa. The absence of impact of P_{O_2} on R_{Acg} means that the amount X^*_{ads} species does not depend strongly on this parameter that is an observation consistent with previous FTIR observations.[7] This means that the rate of oxygen adsorption for $P_{O_2} > 1$ kPa, allows to maintain constant the amount of the X^*_{ads} species. After 2 min of O_2-PCO with 1% O_2/2% Ar/ He (Figure 5B), the UV lamp is turned off: it can be observed that the acetone production decreases more progressively than in Figure 5A, because a fraction of acetone has been accumulated on the s_1 sites liberated by the conversion of the IPA_{sads} species in the absence of IPA_g. When the UV lamp is turned on again, the acetone production increases progressively due to O_2-PCO of IPA_{sads}. However, the maximum of the rate of the acetone production is lower than at the steady state because due to the absence of competition with the IPA_g associated to the removal of IPA_{sads} by O_2-PCO, a larger fraction of acetone remains on the TiO_2 surface. In Figure 5C after the UV lamp is turned off (decrease in the acetone production), a switch 1% O_2/2% Ar/ He → He is performed. It can be observed that the rate of desorption of acetone is not modified by the switch indicating that there is no significant acetone production from the thermal oxidation of adsorbed species.

Evolution on the Coverage of TiO_2 using FTIR Spectroscopy (Static Condition). After the pretreatment of the TiO_2 pellet, IPA_g is introduced at 300 K until an adsorption equilibrium pressure $P_I = 131$ Pa, followed by the introduction of 1.9×10^4 Pa of O_2. After homogenization, the UV lamp is turned on to perform a static O_2-PCO in the presence of gaseous IPA. After 5 min of irradiation, it is observed (results not shown) that (a) the intensity of the IR band at 1467 cm^{-1} remains constant, $\theta_I = 1$, (b) the IR band of Ac_{sads} at 1696 cm^{-1} is detected with a very low intensity indicating a coverage of $\theta_A \approx 0.05$, and (c) P_I decreases to 92 Pa, whereas P_A increases to 39 Pa. θ_A starts to increase significantly only when P_I is very small (for TI ≈ 50 min). This confirms that the TiO_2 surface is not strongly modified in the presence of IPA_g: the competitive chemisorption between IPA_{sads} and Ac_{sads} does not allow the adsorption of acetone even for a low P_I value.

IV. Discussion

The objective of the present study is to provide more insight on the mechanism of the PCO of IPA_g into acetone on TiO_2 using an EMA of the catalytic process. This is an intermediate stage for the interpretation of the deep PCO of IPA into CO_2 and H_2O. To prove the interest of the EMA, we provide a kinetic simulation of the FTIR observations during the O_2-PCO of IPA_{sads} (Figure 1B) using the modified kinetic model M1 and the data from the EMA of the O_2-PCO of IPA.

4.1. Formal Kinetic Data on the PCO of IPA on TiO_2. The formal kinetic data on the O_2-PCO of IPA_g at high θ_I values are (a) the main product is acetone (Figure 4) that is consistent with literature data, the conversion of IPA to acetone is 100% in ref 10 and between 93 and 100% according to the intensity of the UV light in refs 8 and 21; (b) the kinetic orders for IPA and O_2 are 0 for P_I and P_{O_2} values higher than 131 and 790 Pa respectively in agreement with literature data;[10,11] and (c) the rates of oxygen consumption and acetone production correspond to those expected from the stoechiometry of the reaction: IPA + $^1/_2O_2$→ acetone + H_2O (this means that the rate of accumulation of adsorbed oxygenated species is not significant excepted during the first seconds of the UV irradiation Figures 2 and 4).

The 0 kinetic orders for IPA and O_2 are interpreted, by classical formal kinetics, considering that the amount of adsorbed intermediate species are independent of the partial pressures of the reactants. For IPA_g, this implicates that a strongly adsorbed species is formed (IPA_{sads}) with a coverage equal to 1 whatever P_I; this justifies the fact what the EMA study (present study and part I[7]) focuses on the O_2-PCO of IPA_{sads} in the absence of IPA_g. The high selectivity in acetone (there is no significant deep oxidation in the presence of IPA_g) is due to the competitive chemisorption between IPA_{sads} and Ac_{sads} on the s_1 sites. A very small amount of Ac_{sads} can be present on the s_2 sites (≈8% of the total amount of acetone adsorbed on a clean TiO_2 surface). The 0 kinetic order for O_2 (for $P_{O_2} > 790$ Pa) indicates that, in the present experimental conditions, the rate of oxygen adsorption during the UV irradiation allows to maintain constant the amount of X^*_{ads} species during the reaction.

4.2. Modification of the Kinetic Model M1 Considering the Results of the EMA. The plausible kinetic model M1 for the O_2-PCO of IPA supports the design of the experiments linked to the EMA of the catalytic process. However, similarly to previous studies,[2,3] the experimental observations lead to the view that the description of surface elementary steps of model M1 must be modified as detailed below in relationship with the kinetic simulation of the static O_2-PCO of IPA_{sads} (Figure 1B).

Step S1. In the absence of IPA_g (Figure 1B), step S1 is not involved in the kinetic calculation. However, it has been shown that at 300 K the strong adsorption of IPA (948 μmol/g) provides two adsorbed species (nd- and d-IPA_{sads}) on s_1 sites representing $\approx$ 16% of the sites of the TiO_2 surface.[7] In the present EMA study, the reactivity of the two IPA_{sads} species for desorption and PCO are only qualitatively differentiated due to the difficulty to find two distinguishable IR bands characteristic of each species and not overlapped to those of the acetone and formate species. To take into account the number of s_1 sites in the calculations, step S1 is denoted

$$\text{step S1a:}\quad IPA_g + s_1 \rightarrow IPA_{sads}\text{-}s_1 \qquad (0)$$

Step S2. At 300 K, the nd- and d-IPA_{sads} species do not desorb: their activation energies of desorption vary linearly with the coverage from 118 to 178 kJ/mol assuming first kinetic order and a preexponential factor of the rate constant $\nu = kT/h$.[7] Moreover, they are displaced neither by acetone nor by water.[7] This means that step S2 can be neglected in the kinetic model of the O_2-PCO of IPA_{sads}.

Steps S3−S5. They are studied in more detail in a forthcoming paper. However, it has been shown that P_{O_2} values >1 kPa have a significant impact neither on the rate of the O_2-PCO of IPA_g (Figure 3) nor on that of IPA_{sads} (Figure 2) that is consistent with literature data.[10,11] This means that, during the O_2-PCO of IPA_{sads}, the amount of X^*_{ads} species can be considered as constant (i.e., if O_{lat} species are involved in the process,[11,18−20] the readsorption of O_2 is a fast process as compared to the rate of O_{lat} consumption).

Step S6. It is inoperative in the dark at 300 K (the thermal oxidation of IPA_{sads} is neglected in the calculations). During O_2-PCO, the I_{1ads} intermediate species has been identified as Ac_{sads}.[7] Moreover, there is a heterogeneity in the reactivity of the IPA_{sads} species (nd- and d-IPA species) as revealed by the TPD measurements (Figure 3) after different durations of the O_2-PCO of IPA_{sads}: the IPA_{sads} species desorbing as IPA_g (at least a fraction of nd-IPA_{sads}) are more reactive that those producing propylene (d- and possibly nd-IPA_{sads} species transformed into d-IPA_{sads} species during the TPD).

Step S7. This step must be significantly revisited considering the experimental observations. The activation energy of desorption of Ac_{sads} species on a clean TiO_2 surface is lower than that of IPA_{sads}, varying linearly with its coverage θ_A from 87 to 108 kJ/mol at $\theta_A = 1$ and 0, respectively (with a preexponential factor of the rate constant $\nu = kT/h$).[7] On a clean TiO_2 surface, it has been shown that acetone is mainly adsorbed on a fraction of the s_1 sites adsorbing IPA_{sads} and on a small number of specific s_2 sites ($\approx$8% of the total amount of adsorbed acetone).[7] This means that at high θ_I values there is a competitive chemisorption IPA/acetone on the common s_1 sites, leading to the displacement of the Ac_{sads} species. This displacement indicates that the rate of desorption of the Ac_{sads} (step S7) in the presence of IPA_{sads} must be strongly higher than that measured on a clean TiO_2 surface.[7] During O_2-PCO of IPA_{sads}, the impact of the competitive chemisorption can be described as follows: (a) at high θ_I values, the rate of the Ac_{sads} desorption on the common s_1 sites is increased significantly as compared to a clean TiO_2 surface leading to a very low coverage of the Ac_{sads} species, and (b) Ac_{sads} can be formed on the s_2 sites (because there is no competition with IPA_{sads}) via a surface elementary diffusion step from the s_1 to the s_2 sites. This leads to modify step S7 as follows:

$$\text{S6: first L−H step}\qquad IPA_{ads}\text{-}s_1 + X^*_{ads} \rightarrow Ac_{ads}\text{-}s_1 + \Sigma\, Y_{ads} \qquad (1)$$

$$\text{S7a: diffusion from } s_1 \text{ to } s_2:\quad Ac_{ads}\text{-}s_1 \rightarrow Ac_{sads}\text{-}s_2 \qquad (2)$$

$$\text{S7b: desorption due to the competitive chemisorption:}\qquad Ac_{ads}\text{-}s_1 \rightarrow Ac_g + s_1 \qquad (3)$$

Moreover, in static conditions, the significant removal of IPA_{sads} species from the s_1 sites by O_2-PCO leads to a decrease in the competitive chemisorption IPA/Acetone allowing the readsorption of acetone on the free s_1 sites able to adsorb Ac_{sads} (only a fraction of the s_1 sites may adsorb acetone). The nature of this Ac_{sads} species is identical to that provided by step S6. However, to differentiate the mode of formation (readsorption), we adopt a different notation (indice reads)

$$\text{step 7c:}\quad Ac_g + s_1 \rightarrow Ac_{reads} - s_1 \qquad (4)$$

Step 8. This step is similar to step S6 and it represents the O_2-PCO of Ac_{sads} on the s_2 and s_1 sites. We adopt the view that the rate constant of the elementary step S8 is the same, whatever the adsorption sites (s_1 or s_2) of Ac_{sads}. The nature of I_{2ads} coming from the O_2-PCO of Ac_{sads} is not considered in the present study.

4.3. Exploitation of the Modified Kinetic Model M1. The kinetic calculations are performed considering the mean field approximation. The objective is to provide a simulation of the experimental data obtained with the IR cell (static condition) during the O_2-PCO of IPA_{sads} species (Figure 1B): the evolutions of (a) θ_I and θ_A and (b) the partial pressure of acetone P_A. The theoretical evolution of $P_A(t)$ is obtained from the amount of gaseous acetone molecules: $N_{Acg}(t)$ in the IR cell after an UV irradiation duration t

$$P_A(t) = \frac{N_{Acg}(t)kT}{V} \qquad (5)$$

where k is the Boltzmann's constant, T is the temperature, and V is the volume of the IR cell. To obtain $N_{Acg}(t)$ from the modified kinetic model M1, the rate of the different elementary steps must be expressed in molecule/s as detailed below for the rate of step S6. According to the mean field approximation model, the rate of consumption of the IPA_{sads} species during O_2-PCO of IPA_{sads} on the s_1 sites is

$$\frac{-d\theta_I}{dt} = k_6\theta_I\theta_{X^*} \qquad (6)$$

Considering that the amount of X^*_{ads} is constant for $P_{O_2} > 1.9$ kPa (Figure 5 and ref 7), then eq 6 provides

$$\frac{-d\theta_I}{dt} = K_6\theta_I \qquad (7)$$

where K_6 is an apparent rate constant that depends on the experimental irradiation conditions (via the amount of X^*_{ads}) in agreement with the formal kinetic approach of photocatalytic

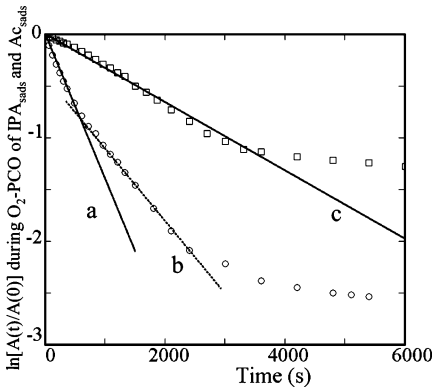

Figure 6. Determination of the apparent rates constants K_6 and K_8 of the elementary steps S6 and S8 (O_2−PCO of IPA_{sads} and Ac_{sads} respectively). (○ and □) Experimental data (FTIR spectra) for IPA_{sads} and Ac_{sads} respectively; (a and b) determination of K_6 for two θ_I coverages; (c) Determination of K_8 (see the text for more details).

processes that shows the rate of reaction is proportional to the radian flux.[22,23] The value of θ_I in eq 7 is provided by

$$\theta_I = \frac{[IPA_{sads-s1}]}{[IPA_{sads-s1}]_F} = \frac{(N_{I-s1})}{(N_{I-s1})_F} \quad (8)$$

where [ ] refers to the surface concentration (molecules/m^2) of the IPA_{sads} species on the s1 sites of TiO_2 and N_{I-s1} is the number of those molecules on the TiO_2 pellet (the subscript F indicates the full coverage). N_{I-s1} is linked to $[IPA_{sads-s1}]$ according to

$$N_{I-s1} = [IPA_{sads-s1}]Sm \quad (9)$$

where S is the BET area (335 m^2/g) and m is the mass of the TiO_2 pellet (0.07 g). This allows one to transform expression (6) to obtain a rate of consumption of IPA_{sads} in molecule/s

$$\frac{-dN_{I-s1}}{dt} = K_6 N_{I-s1} \quad (10)$$

Similar transformations of the different expressions of the rates of the elementary steps of interest are used to obtain a unit in molecule/s.

Determination of the Apparent Rate Constant K_6 of Step S6. During the O_2−PCO of IPA_{sads}, the disappearance of the IPA_{sads} species is provided only by expression (10) (i.e. the rate of desorption is ≈0). The integration of (10) leads to

$$N_{I-s1}(t) = N_{I-s1}(0)\exp(-K_6 t) \quad (11)$$

with $N_{I-s1}(0) = (N_{I-s1})_F$. Expression (10) shows that $\ln[N_{I-s1}(t)/N_{I-s1}(0)] = f(t)$ must be a straight-line with a negative slope providing K_6. In transmission mode, the absorbance of an IR band of an adsorbed species is proportional to its amount on the surface and Figure 6 shows that $\ln[A_{1467cm^{-1}}(t)/A_{1467cm^{-1}}(0)] = f(t)$ is a straight line during the first 20 min of the O_2−PCO (Figure 1): the slope (curve a) provides $K_6 = 1.4 \pm 0.1 \times 10^{-3}$ s^{-1}. The deviation from the straight line for longer duration indicates a decrease in the rate constant of the elementary step S6 in agreement with the difference in reactivity of nd- and d-IPA_{sads} species evidenced by the evolution of the ratio propylene/IPA during TPD observations (Figure 3) after different durations of the O_2−PCO. The slope of the straight-line section after 20 min (curve b in Figure 6) provides $K_6 \approx 0.7 \times 10^{-3}$ s^{-1} for the less reactive IPA_{sads} species.

Determination of the Apparent Rate Constant of Step S8. The rate constant of step S8 has been determined performing the O_2−PCO of Ac_{sads} species similarly to that of IPA_{sads} in Figure 1. Acetone is adsorbed on a pretreated TiO_2 surface and $P_{O_2} = 1.9 \times 10^4$ Pa is introduced after the desorption of the weakly adsorbed species. The progressive disappearance of the IR band at 1696 cm^{-1} is measured with the duration of the UV irradiation (result not shown, described in more detail in a forthcoming article). Curve □ in Figure 6 gives the evolution of $\ln[A_{1696cm^{-1}}(t)/A_{1696cm^{-1}}(0)] = f(t)$ with the duration of the UV irradiation. The rate of disappearance of the Ac_{sads} species is provided by an expression similar to the IPA_{sads} species (expression 10) leading to

$$\frac{-dN_A}{dt} = K_8 N_A \quad (12)$$

where K_8 is the apparent rate of step S8, and N_A is the number of acetone molecules strongly adsorbed on the clean TiO_2 pellet (on the s_2 and a fraction of the s_1 sites). The integration of (12) shows that $\ln[N_A(t)/N_A(0)] = f(t)$ must be a straight line as observed curve c in Figure 6 providing $K_8 = 3.5 \pm 0.1 \times 10^{-4}$ s^{-1}. This value shows that the rate constant of O_2−PCO of Ac_{sads} is lower than that of IPA_{sads} ($K_6/K_8 \approx 4.1$) that is consistent with literature data.[10,13] In particular, Xu et al.[13] in a formal kinetic exploitation of the evolution of IPA_{sads} and Ac_{sads} on TiO_2 P 25 (FTIR measurements) during O_2−PCO of IPA_{sads} consider a ratio of 10. Note that the straight line □ in Figure 6 is observed for longer irradiation durations as compared to IPA_{sads} suggesting that Ac_{sads} species are more homogeneous. This justifies that we assume the same reactivity for the Ac_{sads} species on the s_1 and s_2 sites. However, it is not excluded that the rate constant of step S8 is different for a TiO_2 surface covered by a mixture of IPA_{sads} and Ac_{sads} species.

Evolution of Gaseous and Adsorbed Acetone with the Duration of the Static O_2−PCO of IPA_{sads}. According to the modified kinetic model M1, the intensity of the IR bands of Ac_{sads} species during O_2−PCO is due to three adsorbed species: Ac_{sads}-s_1, Ac_{sads}-s_2, and Ac_{reads}-s_1 (step S7a−S7c). Their net rates (unit in molecule/s) of formation/consumption are provided by the following expressions:

Acetone on the s_1 sites due to the O_2−PCO of IPA_{sads} (steps S6, S7a, and S7b)

$$\frac{dN_{A-s1}}{dt} = K_6 N_{I-s1} - k_{7a} N_{A-s1} - k_{7b} N_{A-s1} \quad (13)$$

Acetone on the s_2 sites due to the diffusion from s_1 (steps S7a and S8)

$$\frac{dN_{A-s2}}{dt} = k_{7a} N_{A-s1} - K_8 N_{A-s2} \quad (14)$$

Acetone re-adsorbed on the s_1 sites liberated by the removal of IPA (step S7c and S8)

$$\frac{dN_{Acreads-s1}}{dt} = \alpha k_a P_A((N_{I-s1})_F - N_{I-s1} - N_{Acreads-s1}) - K_8 N_{Acreads-s1} \quad (15)$$

The factor α is introduced to take into account the fact that only a fraction of the s_1 sites adsorbs acetone (α = 410/948).[7]

The rate of formation of gaseous acetone molecules in the IR cell (step S7a and S7c)

$$\frac{dN_{Acg}}{dt} = k_{7a}N_{I-s1} - \alpha k_a P_A((N_{I-s1})_F - N_{I-s1} - N_{Acreads-s1}) \quad (16)$$

The partial pressure P_A in (15) and (16) is substituted by (5).

4.4. Simulation of the Experimental Data during the O_2−PCO of IPA_{sads} Using the IR Cell. Solving the differential eqs 10 and 13−16 provides the evolutions of number molecules of IPA_{sads} and Ac_{sads} on the TiO_2 surface as well as the partial pressure of the acetone in the IR cell using (5). The differential eq 10 can be solved mathematically providing expression (11). The number of Ac_{sads} on the s_1 sites formed by the O_2−PCO of IPA_{sads}, $N_{Acads-s1}$, can be also obtained by solving mathematically eq 13 using expression (11). However, the rate of formation by step S6 is significantly lower than the rate of consumption by steps S7a and S7b. This means that the approximation of the stationary state can be used in (13) ($dN_{A-s1}/dt = 0$) providing

$$K_6N_{I-s1} - k_{7a}N_{A-s1} - k_{7b}N_{A-s1} = 0$$

$$N_{A-s1} = \frac{K_6N_{I-s1}}{k_{7a} + k_{7b}} \quad (17)$$

The differential eqs 15 and 16 are solved numerically after the substitution using (17) and (11) providing N_{Acg} and $N_{Acreads-s1}$. Figure 7 gives the comparison between the experimental data and the kinetic modeling using the following kinetic parameters:

$K_6 = 1.4 \times 10^{-3}$ s^{-1} from Figure 6.

$k_{7a} = (kT/h)\exp(-E_{dc}/RT)$ from the statistical thermodynamic approach of the adsorption/desorption processes. The activation energy of desorption, E_{dc}, due to the competition between Ac_{sads} and IPA_{sads} on the s_1 sites is not known experimentally. We have shown only that it is significantly lower than that of the desorption of the Ac_{sads} formed on a clean TiO_2 surface (87 kJ/mol at full coverage).[7] Numerous values of E_{dc} significantly lower than 87 kJ/mol can be used in the simulation that selected is E_{dc}= 31 kJ/mol.

$k_{7b} = \nu_{df}\exp(-E_{df}/RT)$, the rate constant of diffusion of the adsorbed acetone on a TiO_2 surface is not known experimentally. However, (a) it is well-known that the activation energy of diffusion is roughly a fraction of that of desorption, $E_{df} = E_dn$ with n the corrugation ratio in the range of 0.1−0.5,[24,25] and (b) the activated complex theory provides an estimation of the preexponential factor in the range of $10^{11}-10^{12}$ s^{-1}.[26] The present kinetic simulation are performed by using $E_{df} = 34$ kJ/mol ($n \approx 0.32$) and $\nu_{df} = 10^{12}$ s^{-1}.

K_8, we have selected a value of the order of magnitude of that determined in Figure 6 and providing the best agreement between experimental and theoretical curve ($k_8 = 6 \times 10^{-4}$ s^{-1} as compared to 3.5×10^{-4} s^{-1} in Figure 6).

k_a, the rate constant of adsorption of acetone on the s_1 sites liberated by the PCO of IPA can be obtained from the statistical thermodynamics[27] assuming (a) nonactivated chemisorption, (b) localized adsorbed species, and (c) neglecting the partition function of rotation and vibration of the gaseous molecules and of vibration of the molecules in the adsorbed state as discussed in more detail in a previous study.[28] This leads to

$$k_a = \frac{h^2}{(2m_a\pi kT)^{3/2}} \quad (18)$$

where m_a is the mass of a molecule of acetone. This leads to $k_a = 3.49$ Pa^{-1} s^{-1}. For a partial pressure of acetone of 34 Pa and for $\theta_I = 0.5$, the theoretical rate of adsorption is ($948 \times 0.5 \times 3.49 \times 34/(350 \times 10^4) = 1.6 \times 10^{-2}$ μmol/(cm²·s), a value strongly higher than the rate of O_2−PCO of the IPA_{sads} species ($948 \times 1.4\ 10^{-3})/(350 \times 10^4) = 3.8 \times 10^{-7}$ μmol/(cm²·s). This high value of the theoretical rate of adsorption means that, except at a coverage of the surface close to the adsorption equilibrium, the experimental rate of adsorption is limited by diffusion processes as discussed in a recent microkinetic study of the CO/O_2 reaction on a Pt/Al_2O_3 catalyst.[29] For instance, considering the theoretical rate of adsorption 1.6×10^{-2} μmol/(cm²·s), the Thiele modulus[30] is $\Phi \approx 10^5$ for a pellet of catalyst ($e_p = 0.025$ cm, density 1.2 g/cm³, porosity of the pellet = 0.46, estimated pore size 7.2 nm, coefficient of effective diffusion ≈0.004 cm²/s). The Thiele modulus provides[30] an effectiveness factor of $\approx 10^{-4}$, indicating that the rate of adsorption is controlled by diffusion processes. Similar calculations for the rate of consumption of O_2 during the O_2−PCO of IPA_{sads} provides $\Phi = 0.07 < 1$ leading to an effectiveness factor of ≈1 indicating that the measurement of K_6 are performed in the absence of mass transport processes as expected for the EMA of a catalytic process. This is also the situation for the measurement of K_8. Considering that the diffusion processes cannot be prevented for the experimental adsorption rate, we use in the present study a value of the apparent rate constant of adsorption k_{ap} significantly lower than that provided by eq 18 and allowing the best agreement between the theoretical and experimental evolutions of the partial pressure of acetone in the IR cell ($k_{ap} = 4 \times 10^{-6}k_a$)

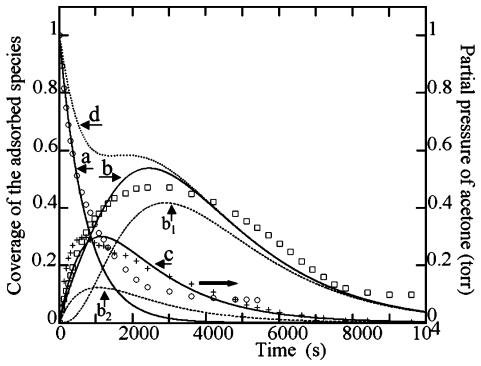

Figure 7. Simulation of the experimental data (FTIR spectroscopy) during the static O_2−PCO of IPA_{sads} considering the experimental microkinetic approach of the catalytic process. (○ and □) Coverages θ_I and θ_A of the IPA_{sads} and Ac_{sads} species; (+) partial pressure of acetone. (a and b) Theoretical evolutions of θ_I and θ_A; (c) theoretical evolution of the partial pressure of acetone; (b_1 and b_2) evolution of the coverage of the s2 and s1 sites by the Ac_{sads} species; (d) evolution of the coverage of the TiO_2 surface by the two adsorbed species (IPA_{sads} and Ac_{sads}).

Figure 7 shows the comparison between experimental and theoretical curves considering the microkinetic model solving eqs 10 and 13−16. These equations provide the numbers of adsorbed species on the TiO_2 pellet that are transformed into coverages by dividing N_{I-s1} by N_{I-s1} (0) and N_{Ac} by the number of acetone that can be strongly adsorbed on a clean TiO_2 surface. Curves b1 and b2 in Figure 7 give the evolution of the coverage of the acetone on the s_1 (readsorption) and s_2 (diffusion process) sites, respectively, whereas curve b obtained from (curve b1 + curve b2) gives the evolution of coverage of the TiO_2 surface by acetone whatever the nature of the sites (it corresponds to the FTIR observations). Curve d provides the sum of the coverage of the IPA_{sads} and Ac_{sads} species. It shows that, during O_2−PCO, the total coverage of the surface is lower than the initial coverage of the IPA_{sads} species whatever the irradiation

duration: the progressive decrease of curve d represents the transformation of Ac_{sads} to CO_2 and formate species (not studied in the present study). Figure 7 shows that the EMA of the O_2-PCO of IPA_{sads} provides theoretical curves that are consistent with the experimental data using the kinetic parameters of interest either determined experimentally (i.e., K_6 and K_8) or estimated considering experimental observations (k_{7a} and k_{7b}).

It must be noted that we have not considered in the kinetic modeling that acetone desorbed from the s_1 sites re-adsorb on the s_2 sites. There are two arguments to justify that this process is neglected (a) the substitution of an adsorption step (similar to step S7c) in place of the surface diffusion step (step S7b) leads to an evolution of θ_A similar to curve b1, however, in Figure 7. However, at $t \approx 0$ the slope of the theoretical curve is equal to 0 at the difference of the experimental data (curve □) and (b) Figures 2 and 4 indicate that there is a delay between the consumption of oxygen and the appearance of gaseous acetone revealing an accumulation of oxygen containing species via a surface process such as diffusion.

To our knowledge, a similar microkinetic approach of the O_2-PCO of IPA_{sads} has not been performed previously. Larson et al.[11] and Xu et al.[13] have performed experiments similar to those of the present study by using MS and FTIR analytical method. However, the kinetic exploitations are mainly descriptive. The single attend to propose a kinetic simulation of the observations is performed by Xu et al.[13] They have shown that the evolutions of the coverages of the IPA_{sads}, Ac_{sads}, and formate species are compatible with a formal kinetic model based on successive first kinetic order reactions

$$A \xrightarrow[k_1]{} B \xrightarrow[k_2]{} C$$

with $k_1/k_2 = 10$ (see Figure 7 in ref 13) that is consistent with our conclusion. However, the authors do not consider the detail of the elementary steps while the formation of gaseous acetone is not involved in the model.

4.5. Exploitation of the Microkinetic Approach of the PCO of IPA. *Comparison between Experimental and Theoretical Catalytic Activity.* This EMA reveals clearly that the superficial process that limits the deep O_2-PCO of IPA_g is the competitive chemisorption between the reactant and the acetone: the desorption of acetone is strongly increased as compared to a clean TiO_2 surface leading to a very small coverage in Ac_{sads} on the common s_1 sites. During the first second of the reaction, Ac_{sads} species can be formed on the small amount of specific s_2 sites by diffusion from the s_1 sites. The high heat of adsorption of the adsorbed IPA intermediate species maintains $\theta_I = 1$ during the reaction in dynamic condition leading to the kinetic order 0 for IPA even for a very low partial pressure of IPA. The competitive chemisorption IPA/acetone explains that gaseous acetone is the main product of O_2-PCO of IPA. This means that the rate of the elementary step S6 must determine the catalytic activity of TiO_2 during O_2-PCO of IPA_g. It has been shown that the apparent rate constant of step S6 is $K_6 = 1.4 \times 10^{-3}$ s^{-1} (Figure 6) that must correspond to the theoretical turnover frequency (TOF_{th}) at high θ_I values. Figure 5 indicates that the rate of acetone production at a low IPA conversion is 12.6 μmol/(g·min) = 0.21 μmol/(g·s). Considering the total amount of IPA_{sads}, 948 μmol/g, this leads to an experimental TOF_{ex} value of 2.2×10^{-4} s^{-1} significantly lower than $TOF_{th} = 1.4 \times 10^{-3}$ s^{-1}. However, it has been shown that nd-IPA_{sads} (desorbing as IPA_g during TPD) is more reactive than the d-IPA_{sads} species for the O_2-PCO process. This may indicate that only the more reactive IPA_{sads} species participates significantly in the formation of acetone at high θ_I values: TOF_{ex} can be calculated using the amount of IPA_g desorbed during a TPD after adsorption of IPA on a clean TIO_2 surface, 232 μmol/g.[7] This leads to $TOF_{ex} = 0.9 \times 10^{-3}$ s^{-1} in reasonable agreement with the theoretical value: 1.4×10^{-3} s^{-1}.

Kinetic Studies for Low IPA Partial Pressures. PCO is a promising process for the removal of organic pollutants in low concentrations in air (from ppb to a few ppm). This explains the numerous studies on the performances of this process for the conversion of various organic molecules. However, the present microkinetic study reveals the difficulties that are expected performing kinetic studies in these experimental conditions. The heat of adsorption of IPA at full coverage is very high 118 kJ/mol. This means that $\theta_I = 1$ even with low partial pressure of IPA, for instance for 0.1 ppm of IPA in one atm of air. However, depending on the ratio gas flow rate/weight of catalysis in the reactor, this coverage can be obtained after a long adsorption duration depending on the IPA content of the reactive mixture. For instance, considering (a) an amount of IPA_{sads} of 948 μmol/g of TiO_2, (b) a gas flow rate of the IPA containing mixture of 100 cm^3/min, and (c) a weight of TiO_2 in a reactor of 0.2 g, then $\theta_I = 1$ is obtained for adsorption durations of 4.6 and 462 min for 1% and 100 ppm of IPA, respectively. For shorter adsorption durations, the coverage of the catalyst sample will be not homogeneous such as $\theta_I = 1$ at the inlet of the reactor and $\theta_I \approx 0$ at the outlet. This means that kinetic studies can be performed under unsteady-state conditions leading to false kinetic conclusions.

Comparisons of the Different TiO_2 Samples. Luo and Falconer[31] have shown that TiO_2 P 25 (a mixture anatase/rutile) presents a reactivity different than a pure anatase TiO_2 sample. This focuses on the impact of the exact natures and amounts of the adsorption sites of the TiO_2 surface. In particular, the present EMA shows that the deep O_2-PCO of IPA is limited by the competitive chemisorption IPA/acetone on a fraction of the s_1 sites of TiO_2 adsorbing IPA. There is no competition on a small amount of s_2 sites specific of the acetone adsorption. It can be understood that if the ratio s_2/s_1 increases due to the composition of the TiO_2 sample then the selectivity CO_2/acetone of the O_2-PCO of IPA may increase.

V. Conclusions

The present experimental microkinetic study has shown that the O_2-PCO of IPA_g, at 300 K, on a pure anatase TiO_2 solid, involves a strongly adsorbed IPA species denoted IPA_{sads}. The process is controlled by the strong competitive chemisorption (on s_1 sites) between the reactant IPA and the product acetone which increases significantly the rate of desorption of acetone. Adsorbed acetone species can be present only on a small amount of specific sites (denoted s_2 representing 8% of the total amount of the TiO_2 sites able to adsorb strongly acetone at 300 K). The competitive chemisorption IPA/acetone limits strongly the deep O_2-PCO of IPA because acetone is the single route for the PCO of IPA into CO_2/H_2O. The catalytic activity (measured in TOF, unit s^{-1}) for the formation of acetone is controlled by the L−H step between the strongly adsorbed IPA_{sads} species and the active oxygen containing species denoted X^*_{ads} formed under UV irradiation: TOF = 1.4×10^{-3} s^{-1}.

In static conditions, it has been shown that the experimental data (coverages of the adsorbed species and partial pressure of acetone) of the O_2-PCO of the IPA_{sads} species can be described using five surface elementary steps

step S6: L−H step under UV irradiation

$$IPA_{sads}\text{-}s_1 + X^*_{ads} \rightarrow Ac_{ads}\text{-}s_1 + \Sigma\, Y_{ads}$$

step S7a: surface diffusion $Ac_{ads}\text{-}s_1 \rightarrow Ac_{sads} - s_2$

step S7b: desorption due to competitive chemisorption

$$Ac_{ads}\text{-}s_1 \rightarrow Ac_g + s_1$$

step S7: readsorption of acetone

$$Ac_g + s_1 \rightarrow Ac_{resads} - s_1$$

step S8: L−H step under UV irradition

$$Ac_{sads} + X_{ads}^* \rightarrow I_{2ads} + \Sigma\, Y_{ads}$$

where X^*_{ads} is an oxygen containing species formed under UV irradiation. The kinetic parameters of each elementary steps of interest have been measured experimentally, and a good agreement has been observed between experimental data and kinetic simulations. In static condition, the coverage of the IPA_{sads} species decreases due to its oxidation into acetone (step S6). This suppresses progressively the competitive chemisorption with acetone (step S7b) and allows (a) the readsorption of acetone (step S7c) and then the deep oxidation via step S8.

Acknowledgment. D.B. acknowledges with pleasure FAURECIA, Systèmes d'échappements, Bois sur prés, 25 550, Bavans, France, for its financial support for the development of the experimental microkinetic approach of catalytic processes

Nomenclature

EMA = experimental microkinetic approach

O_2−PCO and O_{lat}−PCO = photocatalytic oxidation in the presence and in the absence of O_2

IPA_{sads} and Ac_{sads} = strongly adsorbed IPA (two species, nondissociative: nd-, and dissociative d-IPA_{sads}) and acetone species

X^*_{ads} = active oxygen containing adsorbed intermediate species of the O_2−PCO

$QIPA_{sads}$ and QAc_{sads} = amount of adsorbed IPA_{sads} and Ac_{sads} species on the TiO_2 surface

s1 = superficial sites of TiO_2 ($Ti^{+\delta}$ sites with different environments): 948μmol/g, adsorbing IPA (there is a competitive chemisorption with acetone on a fraction α = (410/948) of the s_1 sites)

s2 = superficial $Ti^{+}\delta$ sites of TiO_2 (32 μmol/g) specific of the acetone adsorption.

θ_I, θ_A, and θ_{X^*} = coverage of the TiO_2 surface by IPA_{sads} and Ac_{sads} (with and without competitive chemisorption) and of the X^*_{ads} species

$E_{dI}(\theta_I)$, k_{dI} and $E_{dAc}(\theta_A)$, k_{dAc} = activation energy and rate constant of desorption of IPA_{sads} and Ac_{sads} as a function of the coverage

K_I and P_I and K_A and P_A = adsorption coefficient and partial pressure of IPA and acetone

TOF = turnover frequency for the O_2−PCO of IPA

microkinetic simulation of the static O_2−PCO of IPA_{sads} in the IR cell

t = duration of the O_2−PCO of IPA_{sads}

$N_{Ag}(t)$ = number of acetone molecule in the IR cell

$N_{I-s1}(t)$, $N_{A-s1}(t)$, $N_{A-s2}(t)$ = number of IPA and acetone molecules strongly adsorbed on the s1 and s2 sites of the catalyst pellet ($N_A(t) = N_{A-s1}(t) + N_{A-s2}(t)$)

$N_{Acreads}(t)$ = number of acetone molecules re-adsorbed on the s1 sites

k_y, K_y = rate constant and apparent rate constant of the elementary steps S_y

k_a = theoretical or experimental rate constant for the adsorption of acetone

References and Notes

(1) Dumesic, J. A.; et al.*The Microkinetics of Heterogeneous Catalysis*; ACS Professional Reference Book; American Chemical Society: Washington, DC, 1993.
(2) Bourane, A.; Bianchi, D. *J. Catal.* **2003**, *220*, 3.
(3) Bourane, A.; Bianchi, D. *J. Catal.* **2004**, *222*, 499.
(4) Retailleau, L.; Vonarb, R.; Perrichon, V.; Jean, E.; Bianchi. D. *Energy Fuels* **2004**, *18*, 872.
(5) Vonarb, R.; Hachimi, A.; Jean, E.; Bianchi, D. *Energy Fuels* **2005**, *19*, 35.
(6) Bianchi, D.; Emmanuel, J.; Ristori, A.; Vonarb, R. *Energy Fuels* **2005**, *19*, 1453.
(7) Arsac, F.; Bianchi, D.; Chovelon, J. M.; Ferronato, C.; Herrmann, J. M. *J. Phys. Chem. A* **2006**, *110*, 4202.
(8) Ohko, Y.; Hashimoto, K.; Fujishima, A. *J. Phys. Chem. A* **1997**, *101*, 8057.
(9) Brinkley, D.; Engel, T. *J. Phys. Chem. B* **1998**, *102*, 7596.
(10) Bickley, R. I.; Munuera, G.; Stone, F. S. *J. Catal.* **1973**, *31*, 398.
(11) Larson, S. A.; Widegren, J. A.; Falconer, J. L. *J. Catal.* **1995**, *157*, 611.
(12) Brinkley, D.; Engel, T. *J. Phys. Chem. B* **2000**, *104*, 9836.
(13) Xu, W.; Raftery, D.; Francisco. J. S. *J. Phys. Chem. B* **2003**, *107*, 4537.
(14) Bianchi, D.; Chafik, T.; Khalfallah, M.; Teichner, S. J. *Appl. Catal., A* **1993**, *105*, 223.
(15) El-Maazawi, M.; Finken, A. N.; Nair, A. B.; Grassian, V. H. *J. Catal.* **2000**, *191*, 138.
(16) Bianchi D.; Gass, J. L. *J. Catal.* **1990**, *123*, 298.
(17) Herrmann, J. M. *Appl. Catal., A* **1997**, 1*56*, 285.
(18) Muggli, D. S.; Falconer, J. L. *J. Catal.* **1999**, *187*, 230.
(19) Lee, G. D.; Falconer, J. L. *Catal. Lett.* **2000**, *70*, 145.
(20) Muggli, D. S.; Falconer, J. L. *J. Catal.* **2000**, *191*, 318.
(21) Ohko, Y.; Hashimoto, K.; Fujishima, A. *J. Phys. Chem. B* **1998**, *102*, 1729.
(22) Herrmann, J. M. *Catal. Today* **1999**, *53*, 115.
(23) Herrmann, J. M. *Top. Catal.* **2005**, *34*, 49.
(24) Tompkins, F. C. *Chemisorption of Gases on Metals*; Acadamic Press: London, 1978.
(25) Seebauer, E. G.; Allen, C. E. *Prog. Surf. Sci.* **1995**, *49*, 265.
(26) Hill, T. L. *An Introduction to Statistical Thermodynamics*; Addison-Wesley Publishing Company, Inc: Reading, MA, 1960.
(27) Glasstone, S.; Laidler, K. J.; Eyring, H. *The Theory of Rate Processes*; McGraw-Hill: New York, 1941.
(28) Derrouiche, S.; Bianchi, D. *Langmuir* **2004**, *124*, 116.
(29) Derrouiche, S.; Bianchi, D. *J. Catal.* **2005**, *230*, 359.
(30) Satterfield, C. N.; Sherwood, T. K. *The role of diffusion in Catalysis*; Addison-Wesley Publishing Company, Inc.: Reading, MA, 1963.
(31) Luo, S.; Falconer, J. L. *J. Catal.* **1999**, *185*, 393.